Structure of acetylcholinesterase complexed with the nootropic alkaloid, (–)-huperzine A

Mia L. Raves[1], Michal Harel[1], Yuan-Ping Pang[2], Israel Silman[3], Alan P. Kozikowski[4] and Joel L. Sussman[1,5]

(–)-Huperzine A (HupA) is found in an extract from a club moss that has been used for centuries in Chinese folk medicine. Its action has been attributed to its ability to strongly inhibit acetylcholinesterase (AChE). The crystal structure of the complex of AChE with optically pure HupA at 2.5 Å resolution shows an unexpected orientation for the inhibitor with surprisingly few strong direct interactions with protein residues to explain its high affinity. This structure is compared to the native structure of AChE devoid of any inhibitor as determined to the same resolution. An analysis of the affinities of structural analogues of HupA, correlated with their interactions with the protein, shows the importance of individual hydrophobic interactions between HupA and aromatic residues in the active-site gorge of AChE

(–)-Huperzine A (HupA), an alkaloid isolated from the club moss, *Huperzia serrata*, which has found use in Chinese herbal medicine[1], is a potent reversible inhibitor of acetylcholinesterase (AChE) that lacks potentially complicating muscarinic effects[2,3]. Its unusual pharmacological properties raise the possibility that HupA may be used in symptomatic treatment of disorders believed to involve cholinergic insufficiency[4]. In particular, there is substantial evidence for a role for acetylcholine (ACh) in learning and memory[5], and the cholinergic hypothesis postulates that a cholinergic deficit in Alzheimer's Disease (AD) may be alleviated by cholinesterase inhibitors[6]. Although one AChE inhibitor, tacrine, has been licensed for use in patients with AD[7], and others are at various stages of clinical evaluation[8], the existence of a natural AChE inhibitor, taken together with its unique pharmacological features and relative lack of toxicity[9], render HupA a particularly promising candidate for AD treatment.

Studies on experimental animals reveal significant cognitive enhancement[10], and clinical trials in China have both established the safeness of HupA and provided preliminary evidence for significant effects on patients exhibiting dementia and memory disorders[11]. It was recently demonstrated that HupA decreases neuronal cell death caused by glutamate, particularly in primary cultures derived from hippocampus and cerebellum of the embryonic rat[12]. Its dual pharmacological action suggests that HupA may be a unique and important drug for the treatment of AD patients, since it may serve both to alleviate reduced ACh levels in the brain and to decrease neuronal cell death.

The structure of racemic Huperzine A[13] shows some similarity to other known AChE inhibitors. The molecule is fairly rigid and contains an aromatic system as well as a primary amino group that is probably protonated at physiological pH[14]. It is an optically active molecule, with the naturally occurring (–)-HupA being the more potent of the two enantiomers for both mammalian and *Torpedo californica* AChE (TcAChE)[15,16]. It binds reversibly to fetal bovine serum AChE with a dissociation constant of 6 nM. The affinity for TcAChE is 40-fold lower (K_I=250 nM), and binding to human butyrylcholinesterase is four orders of magnitude weaker (K_I=76 μM)[16].

Visual inspection of HupA reveals no immediate similarity to ACh (Fig. 1). Indeed, various suggestions have been made with respect to its orientation within the active site of AChE, and with respect to the amino acid residues with which its putative pharmacophoric groups might interact[14,16,17]. Solution of the 3D

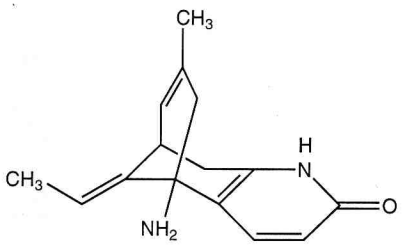

Fig. 1 Structure diagram of optically active Huperzine A. The molecule is chiral, with the (–)-isomer being more potent than either the (+)-isomer or the racemic mixture.

[1]Departments of Structural Biology and [3]Neurobiology, Weizmann Institute of Science, Rehovot 76100, Israel
[2]The Mayo Clinic, Jacksonville, Florida 32224, USA
[4]Institute of Cognitive and Computational Sciences, Georgetown University Medical School, Washington, DC 20007-2197, USA
[5]Department of Biology, Brookhaven National Laboratory, Upton, New York 11973-5000, USA

Correspondence should be addressed to J.L.S.
joel@sgjs3.weizmann.ac.il

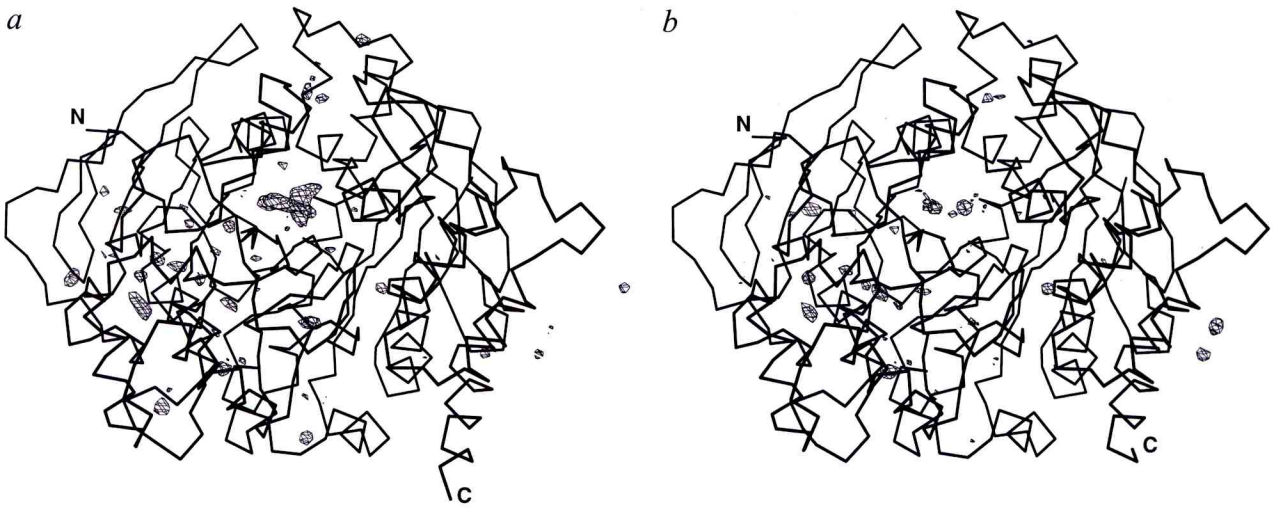

Fig. 2 Cα trace of AChE *a*, in the HupA complex and *b*, in the native protein, showing the initial F_o–F_c maps with 5.0 σ cut-off for all data from 20.0–2.5 Å resolution. The electron density for the HupA molecule is clearly the most prominent feature of the difference map of the complex. Both maps were calculated after a sequence of (i) molecular replacement using the 1ACE structure (resolution 2.8 Å) as a model, (ii) rigid-body and positional refinement, (iii) simulated annealing at 3000 K and (iv) *B*-factor refinement.

structure of a complex of HupA with AChE would permit unequivocal resolution of this issue. Furthermore, it would provide a rational basis for structure-related drug design aimed at developing synthetic analogues of HupA with improved therapeutic properties.

In the following, we report the solution of the structure of a complex of HupA with TcAChE to 2.5 Å resolution, which permitted us to determine the correct orientation and interactions of HupA within the active-site gorge. In addition, the structure of the native enzyme was determined at the same resolution so as to permit accurate pinpointing of the changes in the protein structure brought about by the binding of HupA. The structure of the complex allowed the rationalization of the reported differences in affinity of the ligand for cholinesterases from different species, as well as the different affinities of structural analogues of HupA for AChE.

Structure determination

The highest peak in the initial F_o–F_c maps of the AChE–HupA complex, and two other peaks, at 7.1, 5.6 and 5.6 σ, respectively, were located near the active site, at the bottom of the aromatic gorge. A molecule of HupA was placed in the density around these positions, which roughly resembles its outline. 208 waters were located in F_o–F_c maps, one of which is positioned on the crystallographic two-fold axis, as well as three C-terminal residues that were previously undetermined[18], including Cys 537, which forms a disulphide bond between the two monomers across the crystallographic two-fold axis. The final *R*-factor for the refined structure of the AChE–HupA complex is 20.5% for all data between 8.0–2.5 Å, and R_{free}=24.8%. The r.m.s. deviations from ideality are 0.015 Å in bond lengths and 1.99° in bond angles. Electron density difference maps for the native structure show clearly that the active site of the enzyme is devoid of inhibitor. The native AChE yielded a residual *R*-factor of 19.9% on refinement, with R_{free}=25.8% and 204 waters, including one on the crystallographic two-fold axis. The r.m.s. deviations from ideality for the native structure are 0.014 Å in bond lengths and 1.98° in bond angles.

The initial unbiased F_o–F_c map for the AChE–HupA complex is shown in Fig. 2*a*, alongside a similar map for the native structure (Fig. 2*b*). From comparison of the two maps it is evident that the only prominent electron density in the difference map of the complex is located near the bottom of the active-site gorge[18], with an outline resembling that of HupA. A close-up of this density, displayed at 4.0 σ cutoff, is shown in Fig. 3, with the refined structure of HupA superimposed. Excellent fitting of the molecule to the electron density can be seen.

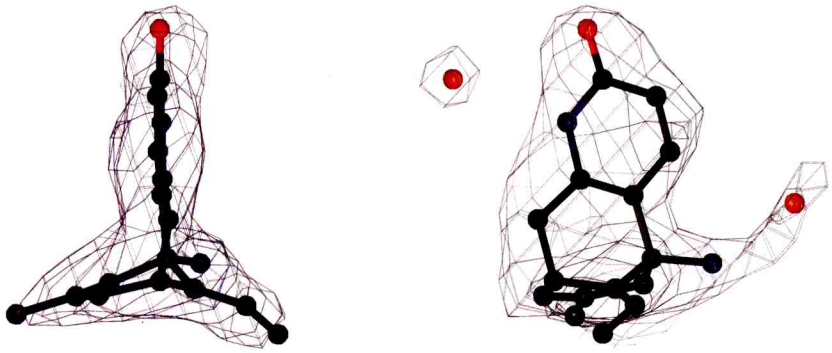

Fig. 3 Two views of the refined structure of HupA in the active site of AChE displayed in the initial F_o–F_c map with 4.0 σ cut-off, showing the excellent fit of the molecule to the electron density.

Protein–ligand interactions

The principal protein–ligand interactions revealed by the refined structure are displayed schematically in Fig. 4. These include: (i) a strong hydrogen bond (2.6 Å) of the carbonyl group of the ligand to the hydroxyl oxygen of Tyr 130; (ii) hydrogen bonds to water molecules within the active-site gorge which are, themselves, hydrogen-bonded to other waters or to side-chain and backbone atoms of the protein, notably to carboxylic oxygens of Glu 199 and to the hydroxyl oxygen of Tyr 121; (iii) interaction of the primary

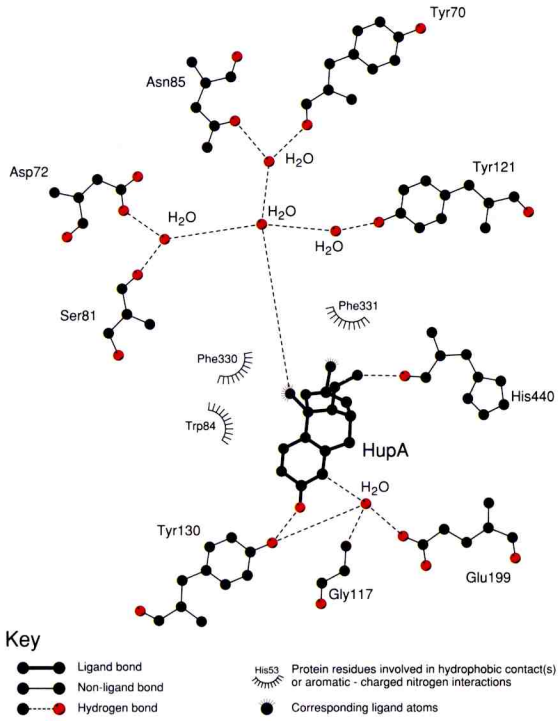

Fig. 4 Schematic figure (using LigPlot[42]) showing the main interactions between the protein and the ligand.

amino group of the ligand, which can be assumed to be charged at the pH of the mother liquor (pH 5.8)[14], with the aromatic rings of Trp 84 and Phe 330, with distances between the nitrogen and the centroids of the rings of 4.8 and 4.7 Å, respectively—this interaction is analogous to that observed for the primary amino group of tacrine[19]; (iv) an unusually short (3.0 Å) C–H•O hydrogen bond between the ethylidene methyl group and the main-chain oxygen of His 440 (a member of the catalytic triad); and (v) several hydrophobic contacts, notably with the side chains and main-chain atoms of Trp 84 and His 440, and with residues Gly 118 through Ser 122.

Fig. 5*a* shows the initial electron-density difference map of HupA within the active-site gorge and the surrounding protein residues. Fig. 5*b* shows the putative waters present in the gorge in the native structure, before the ligand was soaked in, superimposed on the HupA electron density. It can be seen that seven of these waters roughly occupy the place of the ligand. The surrounding residues of the protein retain essentially their original position and orientation.

Native structure

The native structure of TcAChE, determined to a higher resolution (2.5 Å) than the original structure (2.8 Å)[18] is, in fact, of interest not only due to the higher accuracy. The original structure (PDB entry code 1ACE) still contains within its active-site gorge a significant amount of the bisquaternary inhibitor, decamethonium, used for elution from the affinity chromatography resin[20]. Although the presence of various inhibitors within the crystal structure of AChE does not cause a large change in the overall conformation of the protein[19,21], some of the differences observed, especially in the conformations of the side chains of aromatic residues, may be significant. In the present paper, the AChE preparation from which the crystals were obtained was eluted from the affinity resin with the small monoquaternary ligand tetramethylammonium; the electron density ascribed to decamethonium is no longer apparent.

However, the highest peak in the initial electron-density difference map is located at 4.2 Å from the indole ring of Trp 84, close to the position of the proximal quaternary group of decamethonium (PDB access code 1ACL). It is possible that this peak (K0 in Fig. 5*b*) is a (partially occupied) tetramethylammonium or other cationic species, rather than a water molecule. It is of interest that two other prominent peaks in the difference map (K2 and K3, Fig 5*b*), correspond to two of the putative cations (2* and 3* respectively) proposed earlier by Axelsen *et al.*[20] on the basis of molecular dynamics studies. The third putative cation, 1*, is also observed in the structure, but is not in the immediate vicinity of the HupA density and therefore not included in Fig. 5*b*. Wlodek *et al.*[22], on the basis of electrostatic calculations, have suggested that a small cation must be present in the active site of AChE for the enzyme to function. Our structural data are in agreement with these independent theoretical studies which point to a structural and/or functional role for small cations in the active site of AChE.

Comparison of the native coordinates with those for the 1ACE structure shows that the structures are very similar: the r.m.s. deviation in the position of the Cα atoms in the two structures is 0.31 Å. There is only one difference in the configuration of the protein backbone, in the orientation of the peptide bond between residues Pro 165 and Gly 166, which is probably just due to the higher resolution of the maps. A few side chains display a change in conformation, notably Phe 330, in the active site (from $\chi1 = -116°$, $\chi2 = -65°$ to $\chi1 = -160°$, $\chi2 = -85°$), and Trp 279, at the peripheral anionic site (from $\chi2 = 114°$ to $\chi2 = 91°$). These differences are significant, because decamethonium interacts with both residues, influencing their conformations[19]. A few other large side chains, that are not close to the active site, have a slightly different conformation. Based on all

Table 1 Data collection and processing statistics

	HupA	native
Oscillation angle	1.0°	1.0°
No. of frames	90	130
Total no. of observations	334,827	138,332
Average redundancy	5.3	1.9
No. of independent refl.	44,903	46,243
Highest resolution processed	2.3 Å	2.25 Å
Highest resolution in refinement	2.5 Å	2.5 Å
Completeness	99.9%	96.6%
highest resolution shell	99.6% (2.35–2.3 Å)	96.7% (2.33–2.25 Å)
highest resolution used in refinement	100.0% (2.55–2.48 Å)	99.1% (2.67–2.53 Å)
R_{sym}	9.6%	9.5%
highest resolution shell	57.5% (2.35–2.3 Å)	62.1% (2.33–2.25 Å)
highest resolution used in refinement	33.6% (2.55–2.48 Å)	32.3% (2.67–2.53 Å)
Average I / average σ	23.7	7.4
highest resolution shell	3.0 (2.35–2.3 Å)	0.9 (2.33–2.25 Å)
highest resolution used in refinement	5.3 (2.55–2.48 Å)	2.1 (2.67–2.53 Å)

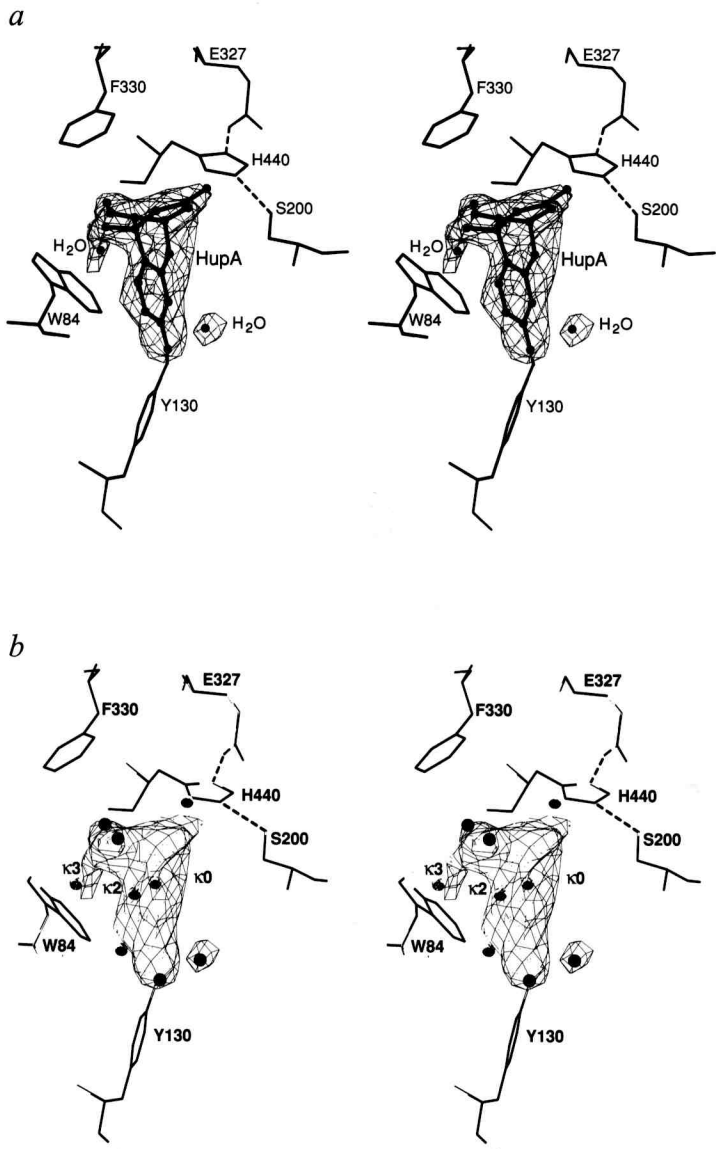

Fig. 5 Stereo views of the initial F_o–F_c map at 4.0 σ around HupA with: *a*, the refined structure of the HupA–AChE complex and two waters in the active site of AChE superimposed; *b*, the same residues in the 2.5 Å native structure and several putative waters in the active site superimposed. K0 roughly occupies the position of the proximal quaternary group of decamethonium (PDB access code 1ACL), K2 and K3 correspond to two of the sites earlier assigned as possible cations[19]. The hydrogen bond between HupA and Tyr 130, and those in the catalytic triad (Ser 200, His 440 and Glu 327) are shown with dashed lines.

inhibitor complexes determined so far, it seems that Phe 330 is the most flexible residue in the protein, as indicated also by the smeared appearance of the electron density for its side chain in the high-resolution native structure.

Docking studies

In our original report on the 3D structure of AChE, we suggested a plausible orientation, obtained by manual docking, of ACh in an all-trans conformation within the active site[18]. In this model, the quaternary ammonium group is positioned directly above the six-membered ring of Trp 84, at 4.1 Å from the nitrogen atom to the centroid of the ring, and at 5.9 Å from Phe 330. In the 2.5 Å native structure, we oriented the modelled ACh molecule so that the acetate moiety retains its position near Ser 200, and the quaternary nitrogen is positioned at 4.8 Å from the centroid of the entire nine-membered indole ring (as the partial charge of the aromatic system is distributed over all nine atoms[23]), so that the distance to the phenyl ring of Phe 330 is now 5.2 Å. Thus, the quaternary ammonium group makes two cation–aromatic interactions. The validity of this model is supported by our X-ray studies of complexes of the enzyme with the reversible inhibitor, edrophonium[19], and with the transition-state analogue, *m*-(*N*,*N*,*N*-trimethylammonio)trifluoroacetophenone[21].

Consideration of its pharmacophoric groups suggests a plausible orientation for HupA parallel to the ACh molecule[24] (Fig. 6*a*). But, in fact, its observed orientation within the active-site gorge appears to be almost orthogonal (Fig. 6*b*). This may explain why several orientations predicted by docking studies were erroneous[14,16]. Saxena *et al.*[16] proposed that the carbonyl group of HupA points towards the putative oxyanion hole and that the primary amino group may interact with the carboxylate of Glu 199. Ashani *et al.*[14] assigned the primary amino group, together with the endocyclic or exocyclic double bonds, as interacting with Trp 86 and Tyr 337 in human recombinant AChE (corresponding to Trp 84 and Phe 330 in TcAChE), and suggested that the pyridone ring heteroatoms form hydrogen bonds to amino acids distal to Tyr 337.

In a docking study using the automated docking program, SYSDOC, three possible orientations of HupA within the active-site gorge were suggested[17]. Binding of HupA to the peripheral site, near Trp 279, was also predicted, but no evidence of that is found in the crystal structure, possibly because the tight packing of the AChE molecules within the crystal produces steric hindrance which precludes binding of ligands to the 'peripheral' site upon soaking[20]. One of the three candidate orientations differs only slightly from that of the crystal structure, inasmuch as it predicts that the pyridone oxygen should be bonded to the main-chain nitrogen of Ser 124 rather than to the hydroxyl group of Tyr 130, with the adjacent ring nitrogen hydrogen-bonding to this hydroxyl instead (Fig. 7). However, this orientation does imply a short distance between the pyridone oxygen and the hydroxyl group of Tyr 130 in the SYSDOC-generated complex.

Binding of HupA analogues

It seems surprising that an inhibitor with such a strong affinity for AChE as HupA binds by means of so few direct contacts. First, even though HupA has three potential hydrogen-bond donor and acceptor sites (Fig. 1), only one strong hydrogen bond is seen, between the pyridone oxygen of the ligand and a protein residue (Fig. 4). Analogous compounds with a methoxy group instead of the carbonyl oxygen show no inhibition at all (Table 2). Second, the ring nitrogen is hydrogen-bonded to the protein through a water molecule, and hydrogen bonds between the $-NH_3^+$ group and the protein are mediated by at least two

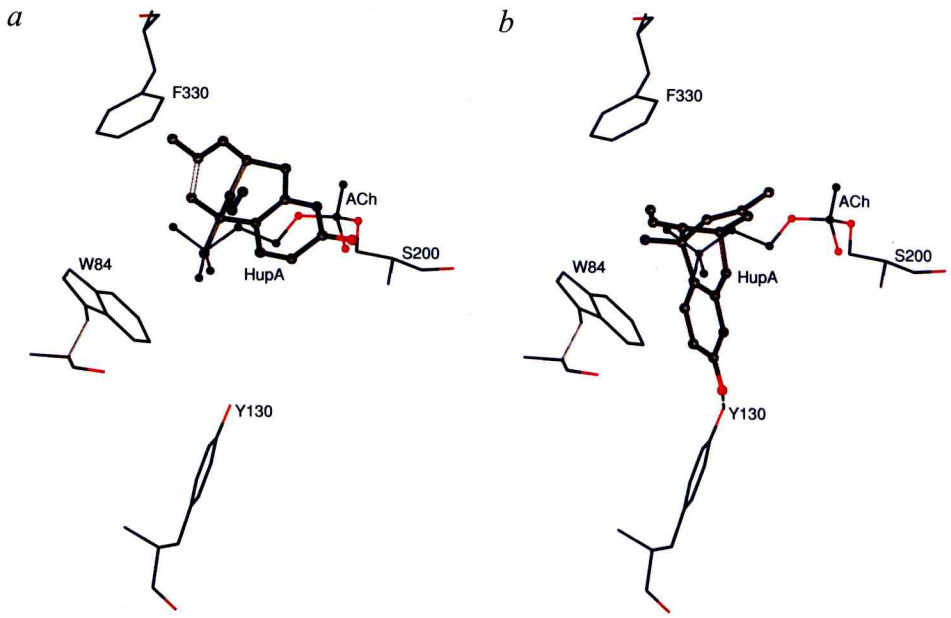

Fig. 6 Orientation of HupA in the active site *a*, based on similarity to ACh and *b*, in this X-ray structure. HupA is shown with thick balls-and-sticks, ACh is shown attached to Ser 200 in the tetrahedral intermediate state, with thin balls-and-sticks.

waters. Third, the aromatic rings of Trp 84 and Phe 330 are near the primary ammonium group, but do not have the preferred tangential orientation that was found in a study of small-molecule structures[25]. Modelling Phe 330 in the crystal structure as a tyrosine, which is the corresponding residue in mammalian AChE, permits the formation of a 3.3 Å hydrogen bond between the hydroxyl oxygen and the primary amino group of HupA. This extra hydrogen bond, together with the cation–π interactions, may explain why HupA binds to mammalian AChE five- to tenfold more strongly than to TcAChE, and only weakly to BuChE, which has no aromatic side chain at this position. Fourth, the short C–H•O hydrogen bond is somewhat unusual, but this type of bonding has previously been reported both in small molecules[26,27] and in proteins[28]. Moreover, the fact that analogue A5 (Table 2)—which differs from HupA only in lacking the methyl group that makes this hydrogen bond—has an affinity that is lower by two orders of magnitude, argues that the interaction is a favourable one, and serves to stabilize HupA in the active-site gorge. Fifth, the crystal structure of the complex shows a large number of hydrophobic interactions: there are 11 contacts between a carbon atom of HupA and oxygen or nitrogen atoms of protein residues and 20 carbon–carbon contacts within 4.0 Å. The exact location of the double bond in the ethylidene tail doesn't seem critical, since the activity of HupC is comparable to that of HupA (Table 2).

There does not appear to be much room for adding additional groups without causing clashes; there is some room near the bridge methyl group, which points into a highly aromatic environment, but not enough for an entire phenyl ring (analogue A7). However, based on modelling studies[29], it was predicted that the addition of a methyl group near the amide group of HupA (analogues A11 and A12, Table 2) should improve binding. Indeed, when this methyl group is in an axial position, the compound displays an eightfold increase in affinity, probably due to extra hydrophobic contacts with Trp 84.

The side chains of residues in the active-site gorge occupy almost identical positions in the native structure and in the complex, and the r.m.s. deviation of Cα atoms between the two structures is 0.30 Å. One major change is observed, however, in the orientation of the peptide bond between Gly 117 and Gly 118 in the so-called oxyanion hole, where the main-chain carbonyl oxygen atom of Gly 117 distinctly points in the opposite direction from that observed in the native structure and in other inhibitor complexes determined so far[19,21,30]. This change in the conformation of the main chain can only have been brought about by the binding of HupA, since the superposition of AChE in the native structure and in the complex shows that the carbonyl groups of Gly 117 and of HupA would be almost parallel if the movement were not to occur, with a close distance of 3.0 Å between the oxygen atoms. We suggest that this peptide flip[31] is

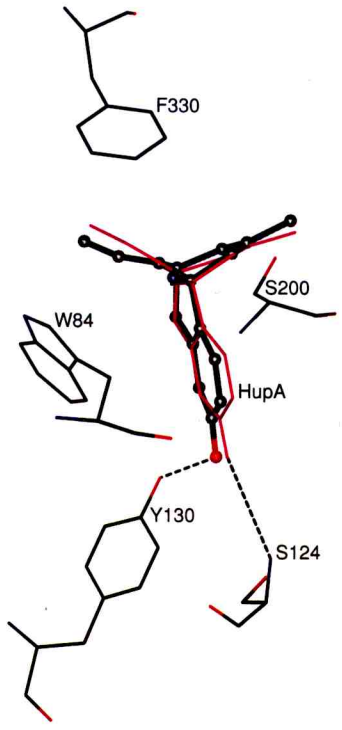

Fig. 7 Orientation of HupA in the active site of AChE obtained in the SYSDOC modelling study performed prior to the determination of the crystal structure of the AChE–HupA complex. The predicted structure (shown in magenta) is almost identical to the X-ray structure (thick balls-and-sticks). For clarity, the molecule in this figure has been rotated by 45° around the vertical (*y*) axis relative to the orientation shown in Figs 5 and 6.

Table 2 Structures and binding affinities of HupA analogues and the differences in interactions with AChE

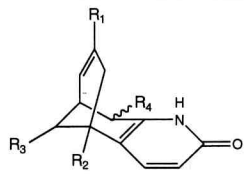

A

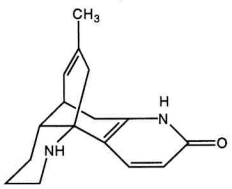

B

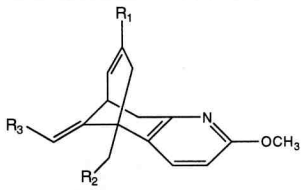

C

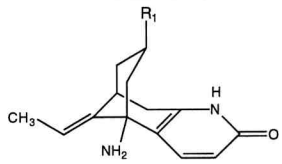

D

	R_1	R_2	R_3	R_4	binding affinity	differences with HupA	ref.
(±)-HupA	$-CH_3$	$-NH_2$	$=CH-CH_3$	-H	$IC_{50}=3\cdot10^{-7}$, $IC^*_{50}=7\cdot10^{-8}$, $K_I=2.4\cdot10^{-8}$ (see footnote)		3, 24, 29, 45
HupC (A1)	$-CH_3$	$-NH_2$	$=CH_2$	-H	comparable to HupA	double bond of R_3 close to Trp 84	43
HupD (A2)	$-CH_2OH$	$N(CH_3)_2$	$=CH_2$	-H	no activity	R_2 clashes with Trp 84, R_1 unfavorable among aromatics	43
Hupi* (A3)	$-CH_3$	$N(CH_3)_2$	$=CH_2$	-H	modest activity	R_2 clashes with Trp 84, double bond of R_3 close to Trp 84	43
A4	$-CH_3$	$-NHCO_2CH_3$	$=CH-CH_3$	-H	$IC_{50}>10^{-4}$	$-OCH_3$ of R_2 clashes with Phe 330, Trp 84 or Ser 122	3, 24,
A5	$-CH_3$	$-NH_2$	$=CH_2$	-H	$IC_{50}=3\cdot10^{-5}$	lacks short C-H · O	3, 24,
A6	$-CH_3$	$-NH_2$	$=CH-CH_3$	-H	$IC_{50}=2\cdot10^{-5}$	R_3 clashes with His 440, Tyr 442 or Phe 330	3, 24,
A7		$-NH_2$	$=CH-CH_3$	-H	$IC_{50}=8\cdot10^{-4}$	R_1 clashes with Phe 290 and Gly 118-Phe 120	3, 24,
A8	$-CH_3$	$-N(CH_3)_2$	$=CH-CH_3$	-H	$IC_{50}=4.5\cdot10^{-4}$	R_2 clashes with Trp 84	3, 24,
A9**	$-CH_3$	$-NH_2$	$-CH=CH_3$	-H	$IC_{50}=6\cdot10^{-6}$	$-CH_3$ of R_3 close to Trp 84	44
A10	$-CH_3$		$=CH-CH_3$	-H	$IC_{50}=1\cdot10^{-3}$	R_2 clashes with Phe 330 or Trp 84	3, 24,
A11	$-CH_3$	$-NH_2$	$=CH-CH_3$	equ. $-CH_3$	$K_I=3.5\cdot10^{-8}$	R_4 points into hydrophilic region	39
A12	$-CH_3$	$-NH_2$	$=CH-CH_3$	axial $-CH_3$	$K_I=3\cdot10^{-9}$	R_4 makes hydrophobic contact with Trp 84	39
HupB (B)					less than HupA	extra ring clashes with Trp 84	44
C1	$-CH_3$	$-N_3$	$=CH-CH_3$		no activity	no H-bond with Tyr 130 possible	3, 29,
C2	$-CH_3$	$-NH_2$	$=CH-CH_3$		no activity	no H-bond with Tyr 130 possible	3, 29,
D1	equ. $-CH_3$				$IC^*_{50}=2\cdot10^{-6}$	ring CH adjacent to R_1 close to Gly 118 Cα	45
D2	axial $-CH_3$				$IC^*_{50}=9\cdot10^{-7}$	R_1 clashes with Gly 117-Gly 119	45
D3	-H				$IC^*_{50}=1\cdot10^{-5}$	ring CH adjacent to R_1 close to Gly 118 Cα	45

All compounds in this table are racemic mixtures
IC_{50} (M) values were measured on rat hippocampal crude homogenate
IC^*_{50} (M) values were measured on rat brain cortex AChE
K_I (M) values were measured on fetal bovine serum AChE
*: Hupi=Huperzinine
**: Z-Huperzine A

the reason for the thus far unexplained slow binding reaction of the inhibitor[32].

In summary, the crystal structure of the HupA-TcAChE complex reveals an unexpected orientation of the ligand within the active site, as well as unusual protein–ligand interactions and a significant change in the main-chain conformation of the protein. This information should be of value for the design and analysis of analogues of HupA with improved pharmacological characteristics.

Methods

TcAChE was purified as described previously[33], with one modification: tetramethylammonium was used instead of the bisquaternary ligand, decamethonium, in the elution of the enzyme from the affinity column, to ensure the absence of the latter inhibitor from the active-site gorge of the purified enzyme[20].

Crystals of native TcAChE were obtained using the hanging-drop vapour diffusion method[34], employing as precipitant 38% polyethyleneglycol 200 in 0.1 M 2-[*N*-morpholino]ethanesulfonic acid, pH 5.8, at 4 °C, and a protein concentration of 12 mg ml^{-1}. For the HupA complex, crystals were soaked for nine days in a solution of ~10 mM optically pure HupA in crystallization mother liquor. X-ray diffraction data for both native and soaked crystals were collected at beam line X11 of the EMBL outstation at the DESY in Hamburg, Germany, on a 30 cm MAR Research image plate detector (λ=0.92 Å). The crystals were cooled to 0 °C using an Oxford Cryosystems cooling device. Both the native crystals and those of the complex diffracted to 2.2 Å, but very weakly at high resolution. The data were processed using DENZO and SCALEPACK[35]. Details of data quality are given in Table 1.

The protein coordinates of the published native structure (PDB entry 1ACE)[18] were used for refinement, which consisted of several cycles of simulated annealing at 3000 K with harmonic constraints for the waters, followed by positional and individual *B*-factor refinement. All

refinement was done using X-PLOR version 3.1[36], employing the Engh and Huber parameters[37]. All data between 8.0–2.5 Å resolution were used in the refinement, and maps were calculated using all data from 20.0–2.5 Å. Coordinates for the racemic mixture of HupA were obtained from the Cambridge Structural Database[13]: only the (–)-stereoisomer gave a good fit to the observed electron density. The molecular geometry of the ligand was constrained during refinement. The density in the HupA complex for the two C-terminal residues, Ala 536 and Cys 537, is weak; the position of the sulphur atom (Cys 537 Sγ), which can be clearly seen, was fixed during initial refinement and released only in the final stage, and the occupancy for the two residues was set to 25%. In the native structure, no connecting density is seen for these two residues. The consistency of the protein geometry and of the positions of the water molecules was validated using ProCheck[38], WhatIf[39] and OOPS[40]. Coordinates and structure factors for both the 2.5 Å native structure and the HupA complex have been deposited at the PDB, and have access codes 2ACE and 1VOT respectively.

For the analysis of the structure-function relationship of various HupA analogues, we generated a series of compounds using InsightII[41], without energy minimization. The molecules so obtained were least-squares fitted to HupA in the crystal structure using the program O[31].

Received 26 September; accepted 25 November 1996.

Acknowledgements

We thank L. Toker for the preparation of the TcAChE, A. Faibusovitch for help in the computations, and K. Wilson and Z. Dauter for their help with the data collection. This research was supported by the U.S. Army Medical, Research and Development Command, the Minerva Foundation, Munich, Germany, the Kimmelman Center for Biomolecular Structure and Assembly, Rehovot, Israel, and the Scientific Cooperation of the European Union with Third Mediterranean Countries through the Israeli Ministry of Science and the Arts. YPP is supported by the Mayo Foundation.

1. Liu, J.-S. *et al.* The structures of huperzine A and B, two new alkaloids exhibiting marked anticholinesterase activity. *Can. J. Chem.* **64**, 837–839 (1986).
2. Wang, Y.E., Yue, D.X. & Tang, X.C. Anticholinesterase activity of huperzine A. *Acta Pharmacol. Sinica* **7**, 110–113 (1986).
3. Kozikowski, A.P., Thiels, E., Tang, X.-C. & Hanin, I. Huperzine A – A possible lead structure in the treatment of Alzheimer's disease. *Adv. Med. Chem.* **1**, 175–205 (1992).
4. Tang, X.C., Xiong, Z.Q., Qian, B.C., Zhou, Z.F. & Zhang, C.L. Cognition improvement by oral Huperzine A: a novel acetylcholinesterase inhibitor, in Alzheimer Disease: Therapeutic Strategies (eds E. Giacobini & R. Becker) 113–119 (Birkhäuser, Boston, 1994).
5. Dunnett, S.B. & Fibiger, H.C. Role of forebrain cholinergic systems in learning and memory: relevance to the cognitive deficits of aging and Alzheimer's dementia. *Prog. Brain Res.* **98**, 413–420 (1993).
6. Becker, R.E. & Giacobini, E. Cholinergic Basis for Alzheimer Therapy (Birkhäuser, Boston, 1991).
7. Davis, K.L. & Powchik, P. Tacrine. *Lancet* **345**, 625–630 (1995).
8. Giacobini, E. & Becker, R. Alzheimer Disease: Therapeutic Strategies (Birkhäuser, Boston, 1994).
9. Laganière, S., Corey, J., Tang, X.-C., Wülfert, E. & Hanin, I. Acute and chronic studies with the anticholinesterase huperzine A: Effect on central nervous system cholinergic parameters. *Neuropharmacology* **30**, 763–768 (1991).
10. Xiong, Z.Q. & Tang, X.C. Effect of Huperzine A, a novel acetylcholinesterase inihibitor, on radial maze performance in rats. *Pharmacol. Biochem. Behavior* **51**, 415–419 (1995).
11. Zhang, R.W. *et al.* Drug evaluation of huperzine A in the treatment of senile memory disorders. *Acta Pharmacol. Sinica* **12**, 250–252 (1991).
12. Ved, H.S., Koenig, M.L., Dave, J.R. & Doctor, B.P. Huperzine A decreases neuronal cell death caused by glutamate. *Neurobiol. Aging*, submitted.
13. Geib, S.J., Tückmantel, W. & Kozikowski, A.P. Huperzine A - a potent acetylcholinesterase inhibitor of use in the treatment of Alzheimer's disease. *Acta Crystallogr.* **47**, 824–827 (1991).
14. Ashani, Y., Grunwald, J., Kronman, C., Velan, B. & Shafferman, A. Role of tyrosine 337 in the binding of huperzine A to the active site of human acetylcholinesterase. *Mol. Pharmacol.* **45**, 555–560 (1994).
15. McKinney, M., Miller, J.H., Yamada, F., Tückmantel, W. & Kozikowski, A.P. Potencies and stereoselectvities of enantiomers of huperzine A for inhibition of rat cortical acetylcholinesterase. *Eur. J. Pharmacol.* **203**, 303–305 (1991).
16. Saxena, A. *et al.* Identification of amino acid residues involved in the binding of Huperzine A to cholinesterases. *Prot. Sci.* **3**, 1770–1778 (1994).
17. Pang, Y.-P. & Kozikowski, A. Prediction of the binding sites of huperzine A in acetylcholinesterase by docking studies. *J. Computer-Aided Mol. Design* **8**, 669–681 (1994).
18. Sussman, J.L. *et al.* Atomic structure of acetylcholinesterase from *Torpedo californica*: a prototypic acetylcholine-binding protein. *Science* **253**, 872–879 (1991).
19. Harel, M. *et al.* Quaternary ligand binding to aromatic residues in the active-site gorge of acetylcholinesterase. *Proc. Natl. Acad. Sci. USA* **90**, 9031–9035 (1993).
20. Axelsen, P.H., Harel, M., Silman, I. & Sussman, J.L. Structure and dynamics of the active site gorge of acetylcholinesterase: synergistic use of molecular dynamics simulation and X-ray crystallography. *Prot. Sci.* **3**, 188–197 (1994).
21. Harel, M., Quinn, D.M., Nair, H.K., Silman, I. & Sussman, J.L. The X-ray structure of a transition state analog complex reveals the molecular origins of the catalytic power and substrate specificity of acetylcholinesterase. *J. Am. Chem. Soc.* **118**, 2340–2346 (1996).
22. Wlodek, S.T. *et al.* in *Enzymes of the cholinesterase family* (eds. Balasubramanian, A.L., Doctor, B.P., Taylor, P. & Quinn, D.M.) 97–104 (Plenum Press, New York, 1995).
23. Dougherty, D.A. Cation-π interactions in chemistry and biology: a new view of benzene, Phe, Tyr and Trp. *Science* **271**, 163–168 (1996).
24. Kozikowski, A.P. *et al.* Synthesis of huperzine A and its analogues and their anticholinesterase activity. *J. Org. Chem.* **56**, 4636–4645 (1991).
25. Verdonk, M.L., Boks, G.J., Kooijman, H., Kanters, J.A. & Kroon, J. Stereochemistry of charged nitrogen-aromatic interactions and its involvement in ligand-receptor binding. *J. Computer-Aided Mol. Design* **7**, 173–182 (1993).
26. Sussman, J.L., Seeman, N.C., Kim, S.-H. & Berman, H.M. The crystal structure of a naturally occurring dinucleotide phosphate uridylyl 3',5'-adenosine phosphate. models for RNA chain folding. *J. Mol. Biol.* **66**, 403–421 (1972).
27. Taylor, R. & Kennard, O. Crystallographic evidence for the existence of C-H...O, C-H....N, and C-H...Cl hydrogen bonds. *J. Am. Chem. Soc.* **104**, 5063–5070 (1982).
28. Derewenda, Z.S., Derewenda, U. & Kobos, P.M. (His) C-H...O=C< hydrogen bond in the active sites of serine hydrolases. *J. Mol. Biol.* **241**, 83–93 (1994).
29. Kozikowski, A.P. *et al.* Identification of a more potent analogue of the naturally occurring alkaloid Huperzine A; predictive molecular modeling of its interaction with AChE. *J. Am. Chem. Soc.* **118**, 11357–11362 (1996).
30. Harel, M., Kleywegt, G.J., Ravelli, R.B.G., Silman, I. & Sussman, J.L. Crystal structure of an acetylcholinesterase-fasciculin complex: interaction of a three-fingered toxin from snake venom with its target. *Structure* **3**, 1355–1366 (1995).
31. Jones, T.A., Zou, J.-Y., Cowan, S.W. & Kjeldgaard, M. Improved methods for building protein models in electron density maps and the location of errors in these models. *Acta Crystallogr.* A**47**, 110–119 (1991).
32. Ashani, Y., Peggins III, J.O. & Doctor, B.P. Mechanism of inhibition of cholinesterases by huperzine A. *Biochem. Biophys. Res. Comm.* **184**, 719–726 (1992).
33. Sussman, J.L. *et al.* Purification and crystallization of a dimeric form of acetylcholinesterase from *Torpedo californica* subsequent to solubilization with phosphatidylinositol-specific phospholipase C. *J. Mol. Biol.* **203**, 821–823 (1988).
34. McPherson, A. The growth and preliminary investigation of protein and nucleic acid crystals for X-ray diffraction analysis. *Meth. Biochem. Anal.* **23**, 249–345 (1976).
35. Otwinowski, Z. Oscillation data reduction program, in Data Collection and Processing, Proceedings of the CCP4 Study Weekend 29–30 January 1993 (eds L. Sawyer, N. Isaacs & S. Bailey) 56–62 (SERC, Daresbury, 1993).
36 Brünger, A.T., Kuriyan, J. & Karplus, M. Crystallographic *R* factor refinement by molecular dynamics. *Science* **235**, 458–460 (1987).
37. Engh, R.H. & Huber, R. Accurate bond and angle parameters for X-ray protein structure refinement. *J. Appl. Crystallogr.* A**47**, 392–400 (1991).
38. Laskowski, R.A., MacArthur, M.W., Moss, D. & Thornton, J.M. PROCHECK: A program to check the stereochemical quality of protein structures. *J. Appl. Crystallogr.* **26**, 283–291 (1993).
39. Vriend, G. WHAT IF: a molecular modelling and drug design program. *J. Mol. Graph.* **8**, 52–56 (1990).
40. Kleywegt, G.J. & Jones, T.A. Efficient rebuilding of protein structures. *Acta Crystallogr.* D**52**, 829–832 (1996).
41. InsightII v. 2.3.0, (Biosym Technologies, San Diego, 1993)
42. Wallace, A.C., Laskowski, R.A. & Thornton, J.M. LIGPLOT: a program to generate schematic diagrams of protein-ligand interactions. *Protein Engng.* **8**, 127–134 (1995).
43. Kozikowski, A.P., Yamada, F., Tang, X.-C. & Hanin, I. Synthesis and biological evaluation of (+/-)-Z-huperzine A. *Tetrahedr. Let.* **31**, 6159–6162 (1990).
44. Kozikowski, A.P. *et al.* Delineating the pharmacophoric elements of huperzine A: importance of the unsaturated three-carbon bridge to its AChE inhibitory activity. *J. Med. Chem.* **34**, 3399–3402 (1991).
45. Liu, J.-S. & Huang, M.-F. The alkaloids huperzines C and D and huperzinine from *Lycopodiastrum casuarinoides*. *Phytochemistry* **37**, 1759–1761 (1994).